Single-shot slightly-off-axis interferometry based Hilbert phase microscopy of red blood cells

Liang Xue, Jiancheng Lai,* Shouyu Wang, and Zhenhua Li

Department of Information Physics and Engineering, Nanjing University of Science and Technology, Nanjing, Jiangsu 210094, China

**laijiancheng@mail.njust.edu.cn*

Abstract: A slightly-off-axis interferometry based Hilbert phase microscopy (HPM) method is developed to quantitatively obtain the phase distribution. Owing to its single-shot nature and details detection ability, HPM can be used to investigate rapid phenomena that take place in transparent structures such as biological cells. Moreover, the slightly-off-axis interferometry owns higher effective bandwidth and more sensitivity than traditional off-axis interferometry. The proposed method takes advantages of the above techniques to obtain the phase image of the red blood cells and compared with the traditional off-axis interferometry and phase retrieval algorithm based on the FFT. The experimental results show that the proposed method owns fine spatial details and real-time imaging ability. We are sure that the proposed method provides a breakthrough for real-time observing and quantitative analyzing of cells *in vivo*.

OCIS codes: (170.0180) Microscopy; (170.1530) Cell analysis; (170.3880) Medical and biological imaging; (180.3170) Interference microscopy.

References and links

1. N. T. Shaked, M. T. Rinehart, and A. Wax, "Dual-interference-channel quantitative-phase microscopy of live cell dynamics," Opt. Lett. **34**(6), 767–769 (2009).
2. D. J. Stephens and V. J. Allan, "Light microscopy techniques for live cell imaging," Science **300**(5616), 82–86 (2003).
3. W. Choi, C. Fang-Yen, K. Badizadegan, S. Oh, N. Lue, R. R. Dasari, and M. S. Feld, "Tomographic phase microscopy," Nat. Methods **4**(9), 717–719 (2007).
4. C. Fang-Yen, S. Oh, Y. Park, W. Choi, S. Song, H. S. Seung, R. R. Dasari, and M. S. Feld, "Imaging voltage-dependent cell motions with heterodyne Mach-Zehnder phase microscopy," Opt. Lett. **32**(11), 1572–1574 (2007).
5. G. N. Vishnyakov and G. G. Levin, "Interferometric computed-microtomography of 3D phase objects," Proc. SPIE **2984**, 64–71 (1997).
6. Y. Sung, W. Choi, C. Fang-Yen, K. Badizadegan, R. R. Dasari, and M. S. Feld, "Optical diffraction tomography for high resolution live cell imaging," Opt. Express **17**(1), 266–277 (2009).
7. Z. Yaqoob, W. Choi, S. Oh, N. Lue, Y. Park, C. Fang-Yen, R. R. Dasari, K. Badizadegan, and M. S. Feld, "Improved phase sensitivity in spectral domain phase microscopy using line-field illumination and self phase-referencing," Opt. Express **17**(13), 10681–10687 (2009).
8. P. Marquet, B. Rappaz, P. J. Magistretti, E. Cuche, Y. Emery, T. Colomb, and C. Depeursinge, "Digital holographic microscopy: a noninvasive contrast imaging technique allowing quantitative visualization of living cells with subwavelength axial accuracy," Opt. Lett. **30**(5), 468–470 (2005).
9. I. Yamaguchi and T. Zhang, "Phase-shifting digital holography," Opt. Lett. **22**(16), 1268–1270 (1997).
10. E. Cuche, P. Marquet, and C. Depeursinge, "Spatial filtering for zero-order and twin-image elimination in digital off-axis holography," Appl. Opt. **39**(23), 4070–4075 (2000).
11. Y. Takaki, H. Kawai, and H. Ohzu, "Hybrid holographic microscopy free of conjugate and zero-order images," Appl. Opt. **38**(23), 4990–4996 (1999).
12. E. N. Leith and J. Upatnieks, "Reconstructed wavefronts and communication theory," J. Opt. Soc. Am. **52**(10), 1123–1128 (1962).
13. N. T. Shaked, Y. Zhu, M. T. Rinehart, and A. Wax, "Two-step-only phase-shifting interferometry with optimized detector bandwidth for microscopy of live cells," Opt. Express **17**(18), 15585–15591 (2009).
14. T. Ikeda, G. Popescu, R. R. Dasari, and M. S. Feld, "Hilbert phase microscopy for investigating fast dynamics in transparent systems," Opt. Lett. **30**(10), 1165–1167 (2005).
15. G. Popescu, T. Ikeda, R. R. Dasari, and M. S. Feld, "Diffraction phase microscopy for quantifying cell structure and dynamics," Opt. Lett. **31**(6), 775–777 (2006).
16. K. Dillon and Y. Fainman, "Depth sectioning of attenuation," J. Opt. Soc. Am. A **27**(6), 1347–1354 (2010).
17. E. D. Taylor, C. Cates, M. E. Mauel, D. A. Maurer, D. Nadle, G. A. Navratil, and M. Shilov, "Nonstationary signal analysis of magnetic islands in plasmas," Rev. Sci. Instrum. **70**(12), 4545–4551 (1999).

#141302 - $15.00 USD Received 18 Jan 2011; revised 1 Mar 2011; accepted 22 Mar 2011; published 29 Mar 2011

18. S. C. Pei and J. J. Ding, "The generalized radial Hilbert transform and its applications to 2-D edge detection (Any direction or specified directions)," in *Proceedings of the IEEE International Conference on Acoustics*, (Institute of Electrical and Electronics Engineers, Hong Kong, 2003), pp. 357–360.
19. "Red blood cell," *http://en.wikipedia.org/wiki/Red_blood_cell*.
20. C. Uzoigwe, "The human erythrocyte has developed the biconcave disc shape to optimise the flow properties of the blood in the large vessels," Med. Hypotheses **67**(5), 1159–1163 (2006).
21. J. Jang, C. Y. Bae, J.-K. Park, and J. C. Ye, "Self-reference extended depth-of-field quantitative phase microscopy," Proc. SPIE **7570**, 757018, 757018-8 (2010).
22. M. Mir, Z. Wang, K. Tangella, and G. Popescu, "Diffraction phase cytometry: blood on a CD-ROM," Opt. Express **17**(4), 2579–2585 (2009).
23. R.Nafe, and W.Schlote, "Methods for shape analysis of two-dimensional closed contours—a biologically important, but widely neglected field in histopathology," Electron J. Pathol. **8**, 022-02 (2002).
24. L. L. Wheeless, R. D. Robinson, O. P. Lapets, C. Cox, A. Rubio, M. Weintraub, and L. J. Benjamin, "Classification of red blood cells as normal, sickle, or other abnormal, using a single image analysis feature," Cytometry **17**(2), 159–166 (1994).
25. N. Lue, J. Bewersdorf, M. D. Lessard, K. Badizadegan, R. R. Dasari, M. S. Feld, and G. Popescu, "Tissue refractometry using Hilbert phase microscopy," Opt. Lett. **32**(24), 3522–3524 (2007).

1. Introduction

Most biological cells, including red blood cells and HeLa cells, are nearly transparent under visible-light illumination and behave essentially as phase objects. Thus, the phase distribution offers the inner structure and dynamics information in the cells in a completely noninvasive manner [1]. Usually, several well-known microscopy techniques have been performed over the past years, such as the phase contrast and differential interference contrast microscopy [2]. However, these general phase microscopy techniques do not yield quantitative phase distribution.

To quantitatively obtain the phase image of the biological cells, the interferometric phase microscopy has been proposed and used in medicine and biology to observe the inner structure of the biological cells [3–7]. The interferometric phase microscopy could provide the quantitative phase images associated with the optical path delays. The optical path delay relates to the cell profile and the refractive index distribution, which can reflect the inner structure and profile of the cells. As a result, the interferometric phase microscopy can make the cellular morphology quantization under real-time condition, and thus can be an important tool for medical diagnostics and cell biology studies [8].

For interferometric phase microscopy, two conventional interferometric methods are presented in the literature: on-axis interferometry [9] and off-axis interferometry [10]. In the case of on-axis interferometry, at least three phase-shifted on-axis interferograms of the sample are required and then the sample phase information is separated through phase-shifting algorithm [11]. However, for dynamic processes, the sample may change between the acquisitions of the multiple frames. In addition, phase noise may increase due to the system fluctuations between the frames. Traditional off-axis interferometry can realize real-time phase imaging, because one can obtain the quantitative phase image from a single interferogram. In the off-axis interferometry, there has a large angle between the reference and sample beams to separate the desired and undesired waves which will lose the sensitivity of interference measurement [12].

In this paper, a hybrid method called single-shot slightly-off-axis interferometry based HPM is demonstrated, which combines the advantages of slightly-off axis interferometry [13], i.e. high effective bandwidth and HPM [14], i.e. single-shot nature and details detection ability. The slightly-off-axis interferometry proposed in Ref. [13]. is an intermediate solution between the conventional on-axis interferometry and off-axis interferometry; it is a powerful tool for interferometric phase measurements of bio-samples with fine spatial details. Our research concerns the use of a single interferogram, in contrast to the two-step phase retrieval algorithms previously used in Ref. [13], so the single-shot Hilbert transform (HT) is employed as the phase retrieval algorithm [14]. In addition, HT inherently allows for robust phase retrieval, which can ensure the accuracy of the phase image. Due to its single-shot nature, HPM acquisition time is limited only by the recording device and thus can be used to accurately quantify nanometer-level path-length shifts at the millisecond time scales or less,

#141302 - $15.00 USD Received 18 Jan 2011; revised 1 Mar 2011; accepted 22 Mar 2011; published 29 Mar 2011

where many relevant biological phenomena develop [15]. To the best of our knowledge, the method proposed in this paper has not been suggested, as it is a hybrid instrument that combines the slightly-off-axis interferometry and HPM for quantitative phase microscopy of red blood cells.

2. Slightly-off-axis interferometry based Hilbert phase microscopy

For slightly-off-axis interferometry, detailed descriptions can be found in Ref. [13]. Briefly speaking, in the spatial frequency spectra of interferometry, two autocorrelation term (ACTs) are located around the origin, and two cross-correlation terms (CCTs), each located on a different side of the spatial frequency domain. But the exact positions of CCTs are decided by the fringe frequency due to the tilt angle between the sample and reference arms. As to the slightly-off-axis interferometry the CCTs should not crossover, but overlap of the ACTs is permitted. Thus, the slightly-off-axis interferometry owns more effective spectral bandwidth than that of off-axis interferometry.

Figure 1 illustrates a possible slightly-off-axis interferometry setup for acquiring only one interferogram. Linearly-polarized light from a 4 mW He-Ne laser (λ = 632.8nm, ϕ = 0.7 mm) is expanded ($M = \frac{f_2}{f_1} = \frac{80}{10} = 8$) and collimated, then split by the modified Mach-Zehnder interferometer. The reference beam is slightly tilted with respect to the sample beam to create a uniform fringe structure. A pair of micro objectives (25× magnification, 0.4 numerical aperture) are used in the sample arm, thus the transmissive confocal system can be described as focusing light with one objective onto the focal plane, then reimaging by a second objective with same focal length [16]. To accomplish the high-speed imaging and collection, the CMOS camera (Mintron, MC1310) has an acquisition rate of 500 frames/s at the full resolution of $1000(\mathrm{H})\times 512(\mathrm{V})$ pixels, with square pixels of 12 μm. For the experiments, the *f*-number of the imaging system is 5.8 and the fringe frequency is set to 17 cycles/mm which meets slightly-off-axis interferometry's demand, depending on the experiment set.

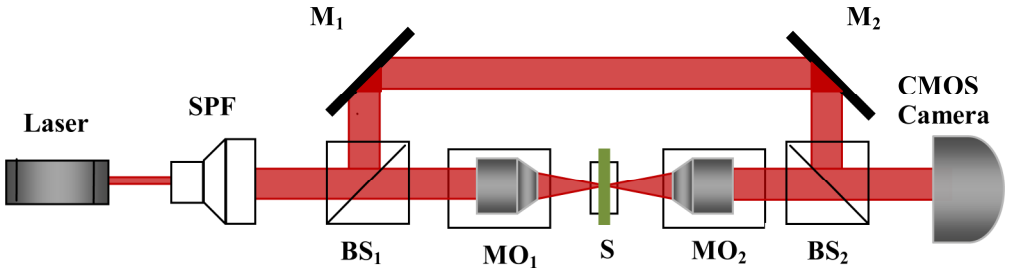

Fig. 1. Experimental setup for slightly-off-axis interference. SPF = Spatial filter (beam expander with a confocally-positioned pinhole), BS_1, BS_2 = Beam splitters; M_1, M_2 = Mirrors; MO_1, MO_2 = Micro objectives; S = Sample.

According to the HPM theory, only one interferogram I is acquired to extract the quantitative phase image. The intensity of the interferogram can be expressed as follows:

$$I(x) = I_R + I_S + 2[I_R I_S(x)]^{1/2} \cos[qx + \phi(x)] \qquad (1)$$

where I_R and I_S are the reference and sample irradiance distributions, respectively, q is the fringe frequency, and ϕ is the spatially-varying phase associated with the measured sample.

The interferogram is Fourier transformed, spatially high-pass filtered to isolate the sinusoidal term $u(x) = 2\sqrt{I_R I_S}\cos[qx + \phi(x)]$ and eliminate the background components, and then the single-shot Hilbert transform of the filtered signal is performed to yield the wrapped phase as follows:

#141302 - $15.00 USD Received 18 Jan 2011; revised 1 Mar 2011; accepted 22 Mar 2011; published 29 Mar 2011

$$z(x) = \frac{1}{2}u(x) + \frac{1}{2}j \cdot HTu(x), \quad \Phi(x) = \tan^{-1}\{\mathrm{Im}[z(x)]/\mathrm{Re}[z(x)]\}, \qquad (2)$$

where HT denotes a Hilbert transform. Note that z exhibits rapid phase modulation with frequency q, and thus Φ is strongly wrapped. Finally, the phase associated with the object is unwrapped by $\phi(x) = \Phi(x) - qx$ [13,14].

To illustrate the advantages of the proposed method, we theoretically analyze the spatial frequency spectra of traditional off-axis and slightly-off-axis interferometry following the example in Ref. [13]. Results show that the traditional off-axis interferometry requires spatial frequency spectral bandwidth at least twice as large as that of the slightly-off-axis interferometry. In other words, the slightly-off-axis interferometry improves the effective bandwidth ratio and makes the best use of bandwidth.

With respect to the phase retrieval algorithm, the traditional method, fast Fourier transform (FFT), needs high carrier frequency. The interferogram is Fourier transformed, spatially filtered to select either positive or negative first order spectrum, and then the inverse Fourier transform of the filtered signal is performed to yield the wrapped phase. The first advantage of the HT to FFT lies in it keeps more high frequency components, that is, more details of bio-sample are restored, including the edge of cells. The second advantage is that the phase retrieval based on FFT is unstable at the high frequency when there exists small errors. However, the phase retrieval based on the HT can robustly calculate the phase distribution. It can quantitatively obtain the phase distribution, even if there are small errors in the interferogram [17]. The third advantage is that the Hilbert transform has higher ability of noise immunity [18]. Most of the other methods may recognize the locations of the noise as the edges. In contrast, when using the HT for edges detection, the noise will be seldom recognized as the edges.

3. Experimental results

3.1. Sample preparation

Mature red blood cells represent a very particular type of structure; they lack nuclei and organelles and thus can be modeled as optically homogeneous objects [14], which significantly simplifies mathematical modeling of quantitative phase images [15]. To demonstrate the instrument's capabilities for cell imaging, rabbit red blood cells were used as the samples, which have a flat, biconcave disc-like shape with a diameter of about $7-8\mu m$ [19]. The cells were cultured in the 0.9% (mass fraction) NaCl solution. An aliquot of this suspension was placed between a slide and cover slip for microscopic analysis.

3.2. Measurements

With the same optical elements, two experimental measurements are executed to capture the interferograms of red blood cells: the traditional off-axis interferometry and the slightly-off-axis interferometry. The first set of experiment, the off-axis case, the fringe frequency should

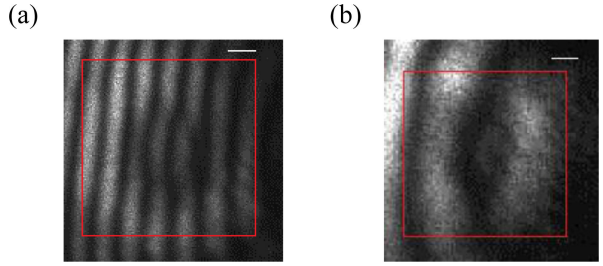

Fig. 2. Interferograms of RBCs (7–8 μm in diameter). (a) Off-axis interferogram. (b) slightly-off-axis interferogram. White horizontal scale bars in (a, b) represent 1 μm.

#141302 - $15.00 USD Received 18 Jan 2011; revised 1 Mar 2011; accepted 22 Mar 2011; published 29 Mar 2011

high enough to separate the ACTs and CCTs, and the best spatial resolution can be achieved when the fringe frequency on the camera is set to the maximum fringe frequency. The second set of experiment, the slightly off-axis case, the angle between the sample arm and the reference arm is adjusted to meet slightly-off-axis geometry's demand and then the interferogram is captured. Figure 2 presents the off-axis interferogram and slightly-off-axis interferogram, respectively.

3.3. Data analysis

To the same interferogram, two phase retrieval methods are adopted: FFT and HT. So, four methods are used to obtain the phase distribution of the red blood cell, relatively. They are traditional off-axis interferometry using phase retrieval based on FFT (method 1), traditional off-axis interferometry using phase retrieval based on HT (method 2), slightly-off-axis interferometry using phase retrieval based on FFT (method 3), and slightly-off-axis interferometry using phase retrieval based on HT (method 4). It's noted that the first two methods process the same interferogram; the same with the last two methods. Four methods compose a group. We operate ten groups of experiments and randomly select three groups [Figs. 3–5] to illustrate the experimental results. Then the third group [Fig. 5] is demonstrated as an example of the following analysis. To exclude the variation influenced by various cell types, cells were from the same origin of cell lines in each group.

Figures 5 (c) and (d) demonstrate the improvements obtained by the slightly-off-axis technique compared with off-axis interference. Quantitative phase reconstruction based on slightly-off axis interferometry reveals the overall structure of the red blood cell as a result of high effective bandwidth ratio, but off-axis mode provides an incomplete outline especially in edges where partial structure is lost [Figs. 5 (a) and (b)]. Comparing Figs. 5 (a/c) with (b/d), one can easily find that the phase image of red blood cells calculated via the phase extraction method based on the FFT has low quality and only provides an outline of circle but the detailed structures are absent, while the method based on the HT can restore the real concave shape of red blood cells in detail, especially the round shape and thin center. HT's higher abilities on details detection and noise immunity are the main reasons. From the completeness of the structure, the smoothness of the shape and the fluctuations in the inner region, phase distribution in Fig. 5 (d) performs better than those in Figs. 5 (a-c) and is more similar to the real image of the red blood cells, which has a biconcave discoid shape (flattened and depressed in the center) with a dumbbell-shaped cross section and a torus-shaped rim on the edge of the disk [20]. In particular, as one can be seen from Fig. 5(l), the min-max phase difference is about 2.5 rad, which is in agreement with Ref. [21].

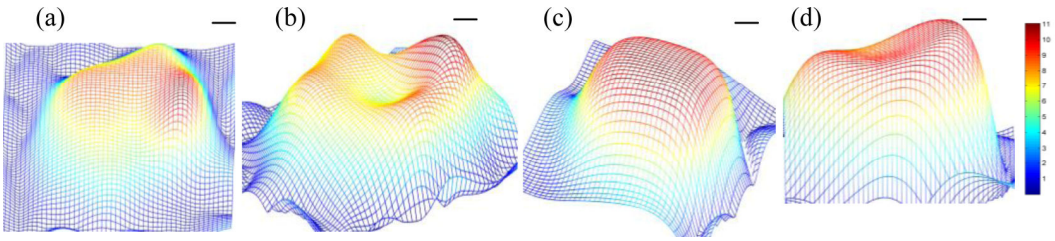

Fig. 3. The first group of quantitative phase images of 7–8 μm red blood cells. (a-d) Final unwrapped phase maps obtained by method 1 to method 4, respectively. Black horizontal scale bars in (a–d) represent 1 μm. The common color bar indicates phase in radians.

#141302 - $15.00 USD Received 18 Jan 2011; revised 1 Mar 2011; accepted 22 Mar 2011; published 29 Mar 2011

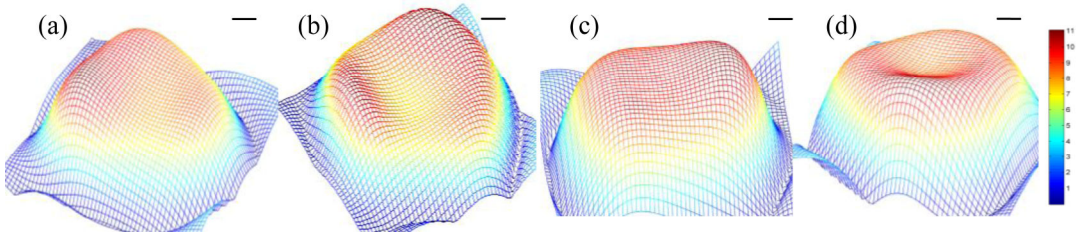

Fig. 4. The second group of quantitative phase images of 7–8 μm red blood cells. (a-d) Final unwrapped phase maps obtained by method 1 to method 4, respectively. Black horizontal scale bars in (a–d) represent 1 μm. The common color bar indicates phase in radians.

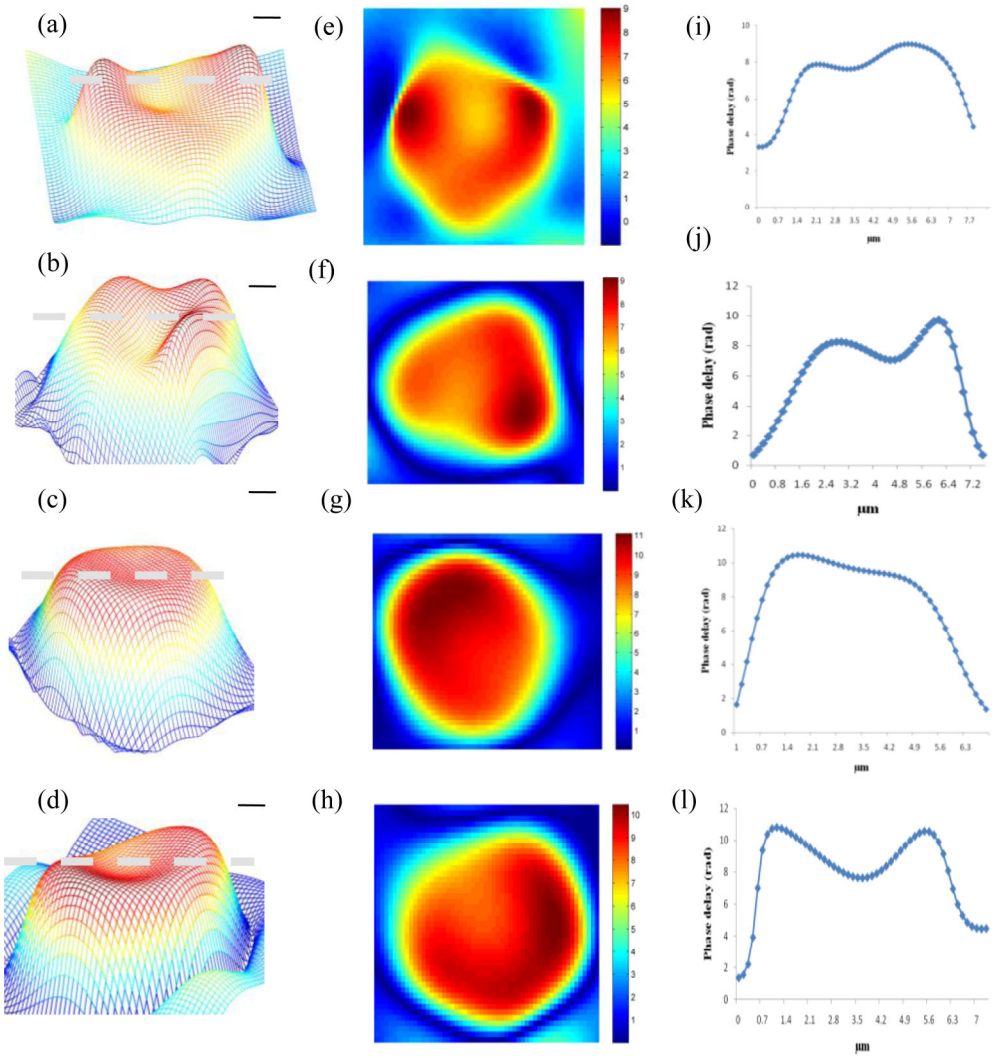

Fig. 5. The third group of quantitative phase images of 7–8 μm red blood cells. (a-d) Final unwrapped phase maps obtained by method 1 to method 4, respectively. Black horizontal scale bars in (a–d) represent 1 μm. It is noted that the first two methods process the same interferogram; the same with the last two methods. (e-h) Vertical views associated with (a-d).The color bars indicate phase in radians. (i-l) Phase profile fluctuations from the dotted line in that crosses the cell in (a-d).

#141302 - $15.00 USD Received 18 Jan 2011; revised 1 Mar 2011; accepted 22 Mar 2011; published 29 Mar 2011

3.3.1. Model parameters to red blood cells

Once the phase images are obtained, we can evaluate the 2-D morphological parameters of cells, such as diameter, projected area, phase histogram, and form factor.

Surface area/ perimeter: The surface area and perimeter of individual red blood cell are evaluated from the phase images and the corresponding results are shown in Table1 [22].

Form factor: It provides a measure of how spherical a cell is, which is calculated as the ratio of the area and the square of the perimeter of the contour [23]:

$$\text{Form factor} = 4 \times \pi \times \frac{\text{Area}}{\text{Perimeter}^2} \tag{3}$$

A perfect circle has a value for this feature of 1.0, whereas the greater the departure from a perfect circle, the lower the value. From the data presented in Table1, we conclude that the form factors of the phase distribution based on the slightly-off-axis interferometry are higher than the off-axis interferometry, and more close to the value 0.878 founded by other method [24].

Table 1. Extracted Image Analysis Features for Each Feature Based on the Consensus Data Set

	Surface Area	Perimeter	Form Factor
Method 1	1100	135	0.76
Method 2	1040	130	0.77
Method 3	1039	124	0.85
Method 4	994	122	0.83

3.3.2. Phase histogram

The phase images of red blood cells appear [Figs. 5(a-d)] qualitatively different. To quantitatively evaluate the quality of the phase image, the phase histograms are calculated and presented in Fig. 6. The size of phase images is 40×40 pixels in total.

As illustrated in Fig. 6, the distribution of these histograms are clearly bimodal, with the first and second peaks relating to the phase shifts of the NaCl solution and cell, respectively. A red dashed line is plotted as a cut line. The average value of the phase associated with the red blood cell is much higher than that of the NaCl solution, which attests that interferometric phase microscopy is indeed sensitive to membrane motions. The data of the second peak on behalf of phase shifts caused by the sample are useful when we analyze the features of bio-sample. So, the cell-to-solution phase value quantity ratio is calculated as Table 2 shows. It's obvious that in the slightly-off-axis geometry more phase information about the cells is retained, because the slightly-off-axis geometry makes full use of the bandwidth.

Furthermore, several important statistical parameters about individual cell can be obtained directly from the histogram (right part of the red dashed line). The standard deviation of phase distribution in the inner of the cell denoted by S_N can be defined as follows:

$$S_N = \sqrt{\frac{1}{N}\sum_{i=1}^{N}(\phi_i - \bar{\phi})^2} \tag{4}$$

where ϕ_i is the phase value of the red blood cell corresponding to each image pixel, $\bar{\phi}$ is the average phase-shift value caused by a single red blood cell, and *N* is the total number of image pixels.

#141302 - $15.00 USD Received 18 Jan 2011; revised 1 Mar 2011; accepted 22 Mar 2011; published 29 Mar 2011

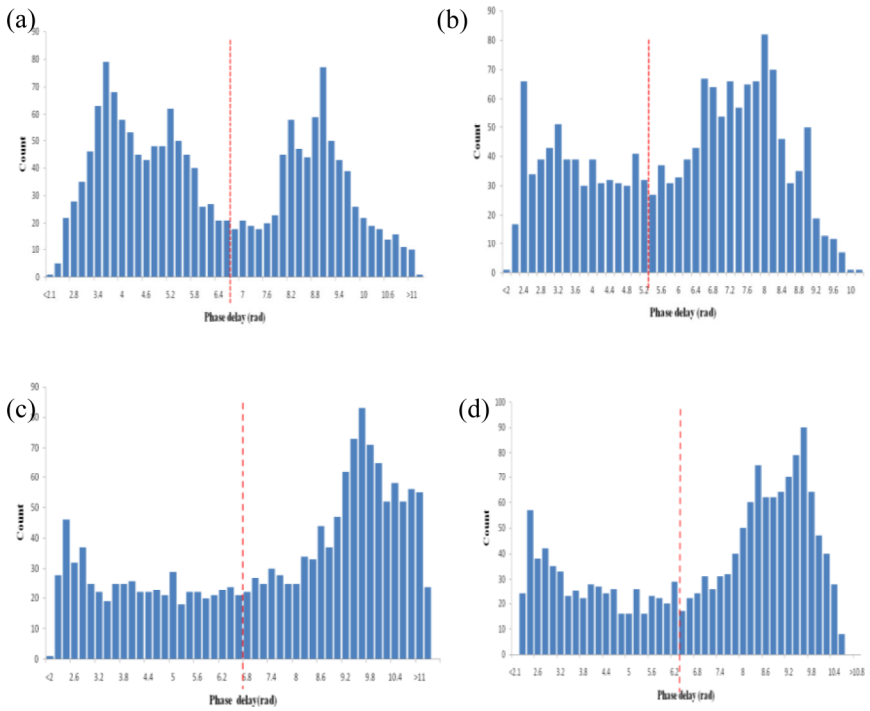

Fig. 6. Corresponding histograms of the phase shifts in Figs. 5 (a-d). The red dashed line is a division, and the left of it represents NaCl solution information while the right part shows cell information.

Table 2. Calculated effective data from the phase histogram

	Cell-to-solution phase value quantity ratio	Standard deviation of phase distribution inside the cell (rad)
Method 1	0.81	0.82834
Method 2	1.44	0.82917
Method 3	1.82	0.79285
Method 4	1.87	0.88069

Four results of S_N corresponding to the four histograms are presented in Table 2. A higher value of S_N represents more fluctuations in the inner of the cell. That is to say, more particulars of the red blood cell itself are reserved. The reason why method 2/4 owns a higher value of S_N than that of method 1/3 is that a high-pass filtering is applied in HT and background components are eliminated while in FFT only first order spectrum is allowed and high-frequency components are lost. In addition, the second phase peak in Fig. 6 (d) has a symmetrical shape which matches the previous literature [25].

3.4. Discussion

The reasons why the slightly-off-axis interferometry performs better are that by applying the traditional off-axis interferometry, high spatial frequencies in the sample field are lost and some noise caused by the experiment cannot be filtered, while slightly-off-axis interferometry method makes full use of the bandwidth and the phase images can better reflect the structure and profile of the red blood cells. Moreover, the Hilbert transform can robustly calculate the phase in the presence of the error in the interferogram. The exact phase distributions can be easily calculated by digitally fitting the background fringes to sine waves, and the temporal phase-shift errors can be avoided. As a result, the single-shot slightly-off-axis interferometry based HPM is better than other methods in sensitivity and effective bandwidth.

#141302 - $15.00 USD Received 18 Jan 2011; revised 1 Mar 2011; accepted 22 Mar 2011; published 29 Mar 2011

4. Conclusion

A single-shot slightly-off-axis interferometry based HPM is developed to obtain the phase image of the biological cells. The method only needs one slightly-off-axis interferogram to extract the phase distribution with no offline measurements and approximations of the sample or the reference fields required. The proposed method is compared with the traditional off-axis interferometry and the phase retrieval method based on the FFT by the experiments. The results show that the proposed method owns high effective bandwidth, fine spatial details and real-time imaging ability. We believe that the proposed method should be a powerful tool for quantitative phase measurements of dynamic processes, especially for observing live biological cell dynamics.

Acknowledgment

This work is supported by the National Natural Science Foundation of China under grants 10704039 and 10904072.

#141302 - $15.00 USD Received 18 Jan 2011; revised 1 Mar 2011; accepted 22 Mar 2011; published 29 Mar 2011